JOURNAL OF SOLID STATE CHEMISTRY 109, 5–14 (1994)

Superstructure and Structural Variants in $Sr_2CuO_2(CO_3)$

O. Milat,*† G. Van Tendeloo,* S. Amelinckx,* T. G. N. Babu,‡ and C. Greaves‡

*EMAT University of Antwerp (RUCA), Groenenborgerlaan 171, B-2020 Antwerpen, Belgium;
†Institute of Physics of the University of Zagreb, Bijenicka 46, POB 304, HR-41000 Zagreb, Croatia; and ‡School of Chemistry, University of Birmingham, Edgbaston, Birmingham B15 2TT, United Kingdom

Received February 16, 1993; in revised form May 6, 1993; accepted May 13, 1993

The structure of the compound $Sr_2CuO_2(CO_3)$ has been reexamined by means of electron diffraction and high resolution electron microscopy. It was found that next to the body centered structure, a second variant of the structure, based on a primitive lattice, occurs. The two structural variants differ in the stacking mode of the CO_3 layers. The actual crystal contains a mixture of these two stacking modes; the body centered one being predominant. A considerable degree of stacking disorder leading to streaked reflections is found mainly in the crystal parts based on the primitive lattice. Under electron irradiation the carbon–oxygen sublattice is found to disorder.

1. INTRODUCTION

One of the main lines in the development of new Cu-based high T_c superconductors consists in doping and substitutions in the "block" layers between which the conducting CuO_2 layers are sandwiched so as to influence the type of carriers and the carrier density in the CuO_2 layer (1). A variety of such block layers was studied for superconductors derived from the prototype $YBa_2Cu_3O_7$ by substitutions in the CuO "chain" layers, mostly of metallic ions. In all of these compounds the square planar CuO_2 layer (or the square pyramidal layer) is the conducting layer. Much less work has been performed along this line on the layered superconductors derived from the prototype La_2CuO_4 in which the conducting layers consist of CuO_6 octahedra. Recently, phases derived from this prototype structure, containing "carbonate layers" have been synthesized (2–4) and $(Sr_{1-x}Ba_x)_2Cu_{1+y}O_{2+2y+z}(CO_3)_{1-y}$ was found to exhibit superconductivity with T_c (onset) $\approx$ 40 K (5); no superconductivity was found in pure $Sr_2CuO_2(CO_3)$. The structure of pure $Sr_2CuO_2(CO_3)$ has been studied by means of X-ray, neutron, and electron diffraction (3, 4). In Ref. (3), the CO_3 groups were found to exhibit orientational disorder, while in (4) it was shown that the CO_3 groups are ordered. In the present paper we confirm the ordering of the CO_3 groups which leads to a body-centered superlattice with unit cell $2a_p \times 2a_p \times 2c_p$, as found in (4), but we show by means of electron diffraction and electron microscopy, that an alternative CO_3 ordering is possible leading to a primitive lattice, with the same unit cell parameters as in (4). We present a model for the CO_3 ordering which accounts for these possibilities and also, we present evidence for the occurrence of long period structures.

2. STRUCTURAL CONSIDERATIONS

The structure of $Sr_2CuO_2(CO_3)$ is related to that of the tetragonal phases $(RE)_2CuO_4$ (6), which themselves are derived from the tetragonal perovskites. According to Ref. (4) the layer sequence in this structure can be represented as: $\cdots$ CuO_2–Sr–CO_3–Sr– $\cdots$. The CuO_2 layers have the usual square planar structure. Along the normal to the layers, i.e., along the c direction the strontium positions project in the centers of the oxygen squares of the CuO_2 layer, which are simultaneously the centers of the copper net. Together with the oxygen atoms belonging to the CO_3 groups, the Sr atoms form puckered SrO layers, of which the oxygen atoms are the apices of CuO_6 octahedra built on the CuO_2 layer. The structure thus contains sandwiches Sr–CuO_2–Sr which are reminiscent of the perovskite blocks in the structures of tetragonal layered high T_c materials and successive sandwich lamellae are separated by layers of CO_3 groups.

In our further discussion of the structural features we shall distinguish the perovskite block layers SrO–CuO_2–SrO and the CO layers (7). The perovskite layers have approximately the tetragonal symmetry of the $(RE)_2CuO_4$ structure with a unit mesh in the layer plane equal to $\mathbf{a}_p^{(1)} \times \mathbf{a}_p^{(2)}$ ($a_p \approx 0.39$ nm). The thickness of one lamella containing a perovskite layer as well as a CO layer is $c_p = 0.75$ nm $\approx 2 \times 0.39$ nm. However, the ordering of the CO (or CO_3) layers decreases the overall translation symmetry as well as the rotation symmetry, and leads to doubling of all lattice parameters, and thus to a unit cell size of $2a_p^{(1)} \times 2a_p^{(2)} \times 2c_p$. In Ref. (4) it was proposed that the unit cell of ordered $Sr_2CuO_2(CO_3)$ is body centered and

0022-4596/94 $6.00

that the space group is $I\bar{4}$. If the CO_3 groups were orientationally disordered or oriented at random, the perovskite lattice symmetry would be preserved as determined in (3, 8).

3. ELECTRON DIFFRACTION PATTERNS, OBSERVATIONS

3.1. General

Electron diffraction patterns along the main zones are reproduced in Fig. 1; they will be discussed with reference to the superlattice unit cell $2a_p \times 2a_p \times 2c_p$.

The [100] (and [010]) zone patterns, Fig. 1a, exhibit a centered rectangular mesh; the diffraction conditions being $k + l$ = even for $0kl$ reflections and $h + l$ = even for $h0l$ reflections.

The [110] (and [1$\bar{1}$0]) zone pattern of Fig. 1b, exhibits the diffraction conditions: hhl present for l = even.

In the [001] zone there are no systematic extinctions. One can distinguish three intensity levels (Fig. 1c). The most intense spots corresponding to the $\mathbf{a}_p^{*(1)} \times \mathbf{a}_p^{*(2)}$ mesh, belong to the basic perovskite structure. The second level of intensity consists of spots situated in the centers of the $\mathbf{a}_p^{*(1)} \times \mathbf{a}_p^{*(2)}$ meshes, suggesting a $a_p\sqrt{2} \times a_p\sqrt{2}$ lattice. The very weak spots divide the edges of the squares of the most intense spots leading finally to a mesh in direct space of $2\mathbf{a}_p^{(1)} \times 2\mathbf{a}_p^{(2)}$. These very weak spots were apparently overlooked in Ref. (4); in $BaSrCuO_2(CO_3)$ the subset of very weak spots was disregarded as being due to double diffraction (9). However, in the [001]* diffraction pattern in Fig. 1c, they cannot be dismissed as being due to double diffraction. Namely, after electron irradiation this subset of the weakest spots tends to disappear presumably due to disordering of the light carbon and oxygen atoms. The disappearance of the weakest spots due to the disordering effect of the electron beam is strikingly illustrated by comparing the [111] zone diffraction pattern before (Fig. 2a) and after electron irradiation (Fig. 2b), in the microscope. These observations suggest strongly that the superstructure with unit mesh $2\mathbf{a}_p^{(1)} \times 2\mathbf{a}_p^{(2)}$ must be related to ordering in the CO layers.

The most instructive patterns are those along $[hk0]$ zones with $h \neq k$; the [310] and [210] zone patterns are reproduced in Fig. 3.

The electron diffraction patterns along these zones exhibit a variability in certain details, depending on the selected area and on the crystal fragment studied (and on the beam-irradiation time). The differences mainly consist in the presence or absence of more or less prominently streaked superstructure reflections, which are visible in zones of the type $[hk0]$ with $h \neq k$. We shall first describe the more complete patterns, and subsequently point out the differences with the simpler patterns.

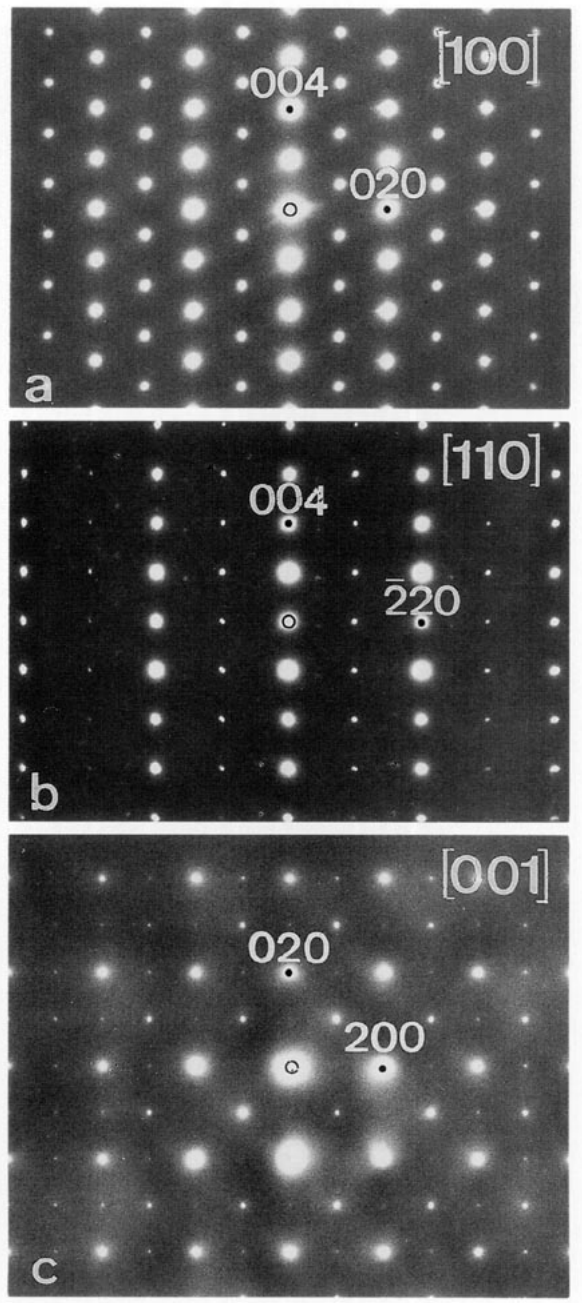

FIG. 1. Electron diffraction patterns of $Sr_2CuO_2(CO_3)$ along the three main zones: (a) [100] zone; (b) [110] zone; (c) [001] zone. Spots marked by dots belong to the mesh of the basic perovskite lattice. In (a) and (b) all spots with $h + k + l$ = odd are absent; in (c) weak spots with $h + k + l$ = odd are present.

3.2. Primitive Lattice

In the [3$\bar{1}$0] zone pattern, Fig. 3a, the [13l]* row consists of an alternation of sharp and diffuse spots; for l = even the spots are sharp; for l = odd they are streaked. In the [26l]* row only sharp spots are observed for l = even; the spots with l = odd are apparently absent.

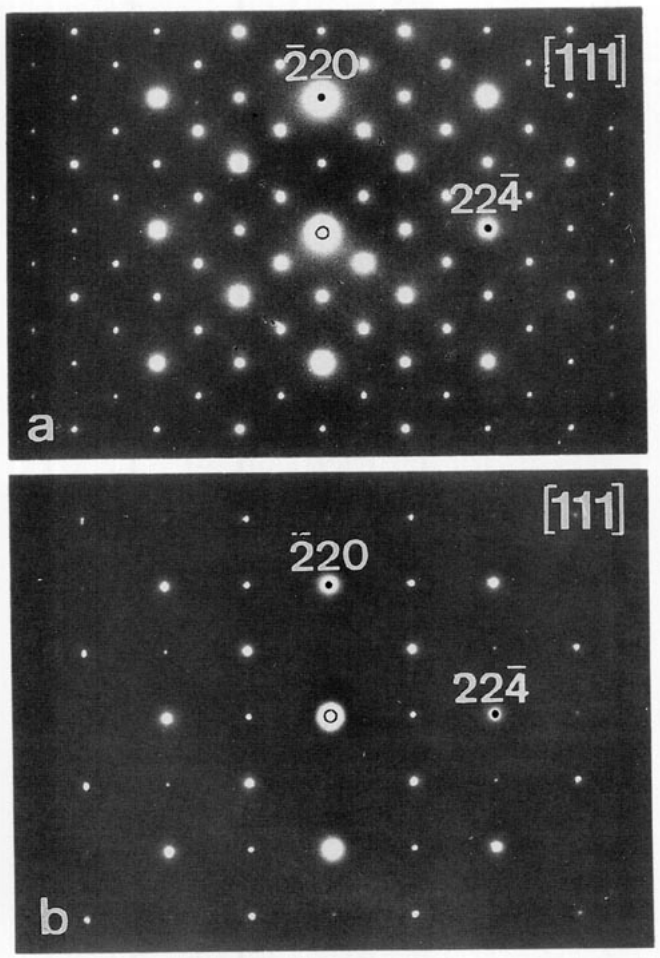

FIG. 2. [111] zone electron diffraction pattern of $Sr_2CuO_2(CO_3)$: (a) before irradiation by the electron beam; (b) after irradiation; a number of weak superlattice spots have disappeared due to disordering of carbon and oxygen atoms in CO layers.

The $[2\bar{1}0]$ zone pattern, Fig. 3b, does not show any systematic extinctions but in each row of spots parallel to $\mathbf{c}^*$, there is again an alternation of sharp and streaked spots. In the $[12l]^*$ row the spots with l = even are diffuse and those with l = odd are sharp; the opposite is true in the $[24l]^*$ row. The streaking in the $[00l]^*$ row must be due to double diffraction since these streaked spots are absent along the $[00l]^*$ row in the [110] zone pattern (Fig. 1b).

We note that the streaked reflections are sometimes absent or scarcely discernible, as in Fig. 3c, but also, that they often consist of closely spaced sharp spots (Fig. 3d) showing that a long period structure is present along the c direction.

The diffraction patterns thus confirm that the lattice has a unit cell of $2\mathbf{a}_p^{(1)} \times 2\mathbf{a}_p^{(2)} \times 2\mathbf{c}_p$, but the diffraction conditions in general, do not seem to be consistent with the body centered unit cell as proposed in (4); in particular, the very weak spots in the [001] zone (in Fig. 1c) and the diffuse spots in the $[hk0]$ zones (in Figs. 3a,b) do not agree with the diffraction condition $h + k + l = 2n$. The diffuse spots occur for $h + k + l$ = odd.

On the other hand the [100], [010], [110], and $[1\bar{1}0]$ zones are in agreement with a body centered unit cell. We shall explain the apparent contradiction below.

3.3. Body-Centered Lattice

In the majority of crystal fragments the streaked reflections are very weak or even completely absent (Fig. 3c); in this case all reflections satisfy the diffraction conditions $h + k + l = 2n$. The lattice may thus be considered as body-centered and the diffraction conditions are consistent with the space group $I4$, found by means of X-ray and neutron diffraction in Ref. (4).

4. STRUCTURAL MODEL

The model for the structure of the SrO–CO–OSr (or Sr–CO_3–Sr) lamella is represented in Fig. 4. In this model the planar CO_3 groups are situated in planes perpendicular to the CO layers and oriented in such a way that one C–O bond is parallel to the layer plane and parallel to a cube direction of the perovskite block. The other oxygen atoms of the CO_3 groups, which share apical positions with the CuO_6 octahedra in two adjacent perovskite layers, are situated on a line perpendicular to the layer planes and passing through the copper positions. The carbon atom is located in the center of the three oxygen atoms which form an equilateral triangle. In the middle plane of a layer the "CO loops", as we shall call them, form a square arrangement, Fig. 4c.

We note at this stage that a "sense" can be attributed to the CO loops; the C–O bonds associated with the four corners of the square all point in the same sense when progressing along the square's periphery. We shall call the CO loop of Fig. 4a, a "− loop"; similarly, a "+ loop" is represented in Fig. 4b.

In the structure, as determined in Ref. (4), the CO_3 triangles are distorted and positioned in such a way that carbon atoms are very close to the special positions, at the square corners of here defined CO loops, i.e., at $\delta' = \frac{1}{4}$ in Fig. 4c. The same arrangement of CO loops was found in all CO layers, but it is shifted over a vector $\frac{1}{2}$ [111] in successive layers leading to body centering.

This can also be the case in the idealized model structure described here in which, deformations of the CO_3 triangles (and of the CuO_6 octahedra) found in (4), are ignored, Fig. 5a and 5c. However, the two CO loops: + loop and − loop, can both be fitted equally well onto the same perovskite block-layer framework leading to deviation from the body centered structure (Figs. 5b,c).

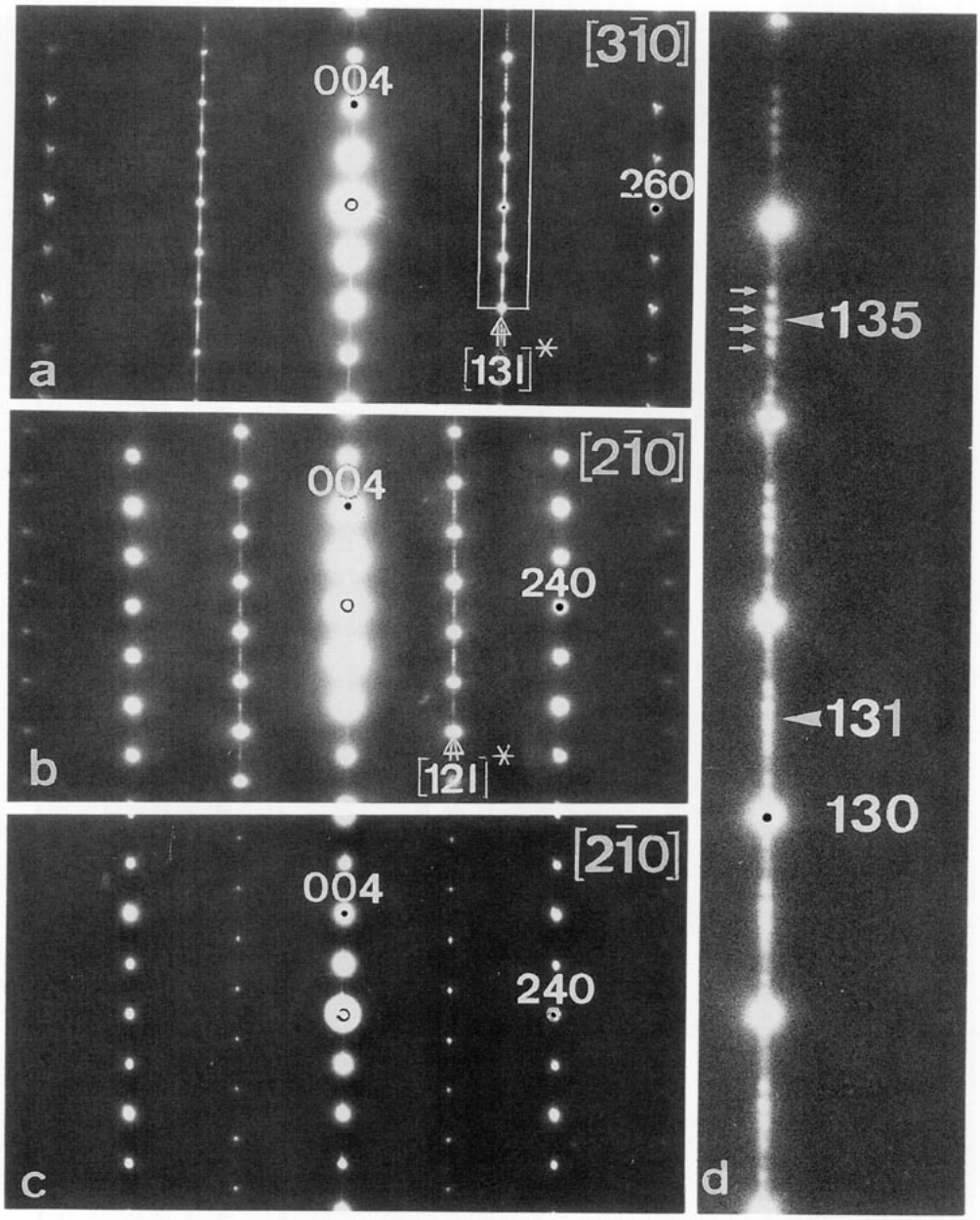

FIG. 3. Electron diffraction patterns of $Sr_2CuO_2(CO_3)$ along "oblique" zones: (a) [310] zone: note the presence of streaked reflections in [13l]* row for $l \neq 2n$ ($h + k + l$ = odd, primitive lattice). The indicated sequence of spots in [13l]* row is enlarged in (d); (b) [2$\bar{1}$0] zone: note the presence of streaked reflections in [12l]* row for $l = 2n$ ($h + k + l$ = odd, primitive lattice); (c) [210] zone: only sharp spots for $h + k + l$ = even (body centered lattice) are present; no streaked spots in [12l]* row, compare this pattern with (b); (d) magnified reproduction of spots in the rectangle in (a) revealing the fine structure of the [13l]* row of reflections. Note the satellite sequences associated with the positions $h + k + l$ = odd.

The structures of "+ CO loop" and "− CO loop" are related by symmetry elements of the perovskite block, i.e., by the mirror operations with respect to the $(100)_p$, $(010)_p$, $(110)_p$, and $(1\bar{1}0)_p$ planes. This means that both arrangements are energetically equivalent and thus, should occur with the same a priori probability and therefore, with the same abundancy, either in the same crystal structure or in separate domains.

According to this model the splitting of the "z" coordinates for the Sr atoms found in (4, 9) can be related to the three different relative positions of the Sr atoms with respect to the CO loops. Namely, from Fig. 5 it is obvious that each Sr atom in a layer above and below a CO layer is either: (i) above (or below) the center of one CO loop, or; (ii) above (or below) the midpoint halfway between two neighboring CO loops, or; (iii) above (or be-

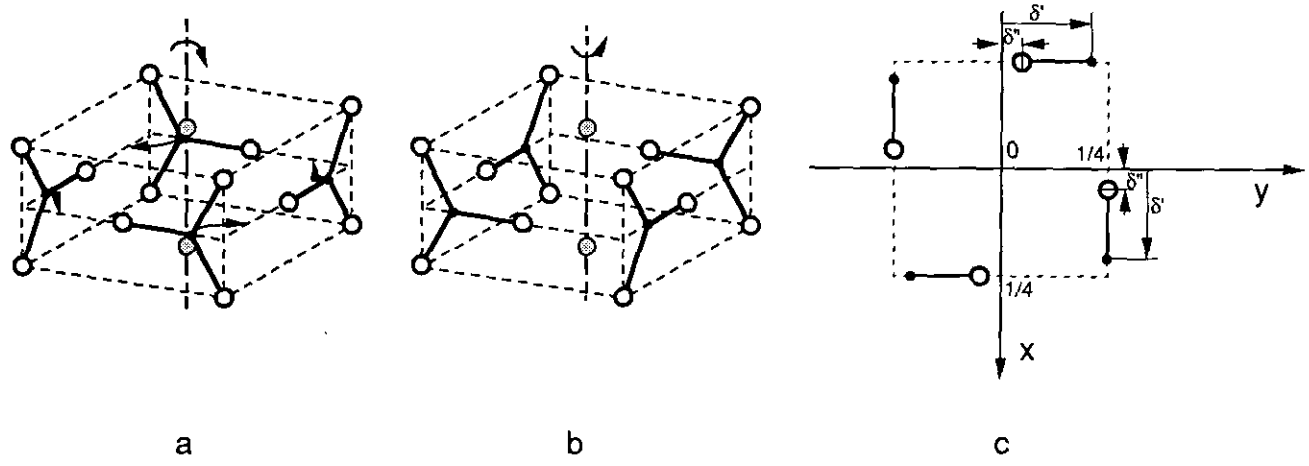

FIG. 4. Arrangement of the CO_3 groups in the lamella Sr–CO_3–Sr of the $Sr_2CuO_2(CO_3)$ structure. The C–O bonds parallel to the c plane point consistently in one sense for all carbon atoms along the periphery of the squares; (a) − CO loop; (b) + CO loop. The arrows in (a) indicate correlation between + and − loops; (c) general positions of carbon and oxygen atoms in a + loop, illustrating the meaning of the symbols δ' and δ'' used in the text; full, shaded, and open circles represent C, Sr, and O atoms, respectively.

low) a point in the center of four neighboring CO loops. These three types of Sr–CO loop configurations are independent of the "sense" of the CO loop. As a consequence, the atoms in the Sr layers become slightly displaced as it is indicated in Fig. 5. The Sr layers become puckered and the periodicities in the "perovskite" SrO–CuO_2–SrO block layers are doubled; therefore the unit cell of this block layer lattice becomes body centered with the parameters: $2a_p \times 2a_p \times 2c_p$.

It is also worth noting that a "+ loop" can be transformed into a "− loop" by the correlated "flipping" of the CO_3 triangles around the square as indicated by arrows in Fig. 4a; the oxygen atoms achieve approximately the same positions on a square. It is also possible to imagine disordered configurations resulting from disorder in the carbon–oxygen sublattice.

The geometry of the CO layers is of prime interest for the interpretation of disorder in this material, which, as we shall demonstrate, is often observed. We shall also show that the crystal structure actually contains both types of CO loops (Fig. 5).

One should note that the CO loops of a given sign can occupy four positions differing by vectors $\frac{1}{2}[100]$, $\frac{1}{2}[010]$, and $\frac{1}{2}[110]$. Of course in any given layer only one position can be occupied. From the fact that the lattice has parameters $2a_p \times 2a_p \times 2c_p$ it follows that within each CO layer all CO loops must be oriented in the same sense, since otherwise a larger mesh size would result in the [001] zone, unless the CO loops would be oriented at random. The tetragonal symmetry further requires that the CO layers are either aligned along the c direction, or that a "loop" in one layer projects in the center of four loops in the adjacent layer (Fig. 5).

5. INTERPRETATION OF THE DIFFRACTION PATTERNS

As a preliminary for the discussion of the diffraction patterns we consider the structure factor of the CO loop. We refer the CO loop to a reference system with its origin in the center of the square, Fig. 4c; the positions of atoms in a "+ loop", are then:

$$\text{C: } \tfrac{1}{4}, -\delta'; \delta', \tfrac{1}{4}; -\tfrac{1}{4}, \delta'; -\delta', -\tfrac{1}{4};$$

$$\text{O: } \tfrac{1}{4}, -\delta''; \delta'', \tfrac{1}{4}; -\tfrac{1}{4}, \delta''; -\delta'', -\tfrac{1}{4};$$

where δ' and δ'' are the coordinates of C and O atoms, respectively. This allows to describe a general position of the CO_3 triangles including also the two special cases: (i) for $\delta' = \frac{1}{4}$ and $\delta'' = \frac{1}{12}$, the carbon atoms occupy special sites at the corners of the CO loops vertically above Cu atoms in the CuO_2 planes, as suggested in (3, 4) (the CO_3 triangles and CuO_6 octahedra being distorted); (ii) for $\delta' = \frac{1}{6}$ and $\delta'' = 0$, the oxygen atoms, forming vertical edges of the CO_3 triangles, occupy special positions above and below the corners of the CO loops, in-line with the Cu atoms in the CuO_2 planes, as represented in Figs. 4a,b, and in Fig. 5. In this latter, idealized case, the CO_3 triangles and CuO_6 octahedra would remain undistorted. The structure factor for the + loop is then generally:

$$F = 2f_C\left\{\cos\left[\frac{\pi}{2}(h - 4k\delta')\right] + \cos\left[\frac{\pi}{2}(4h\delta' + k)\right]\right\} + 2f_O\left\{\cos\left[\frac{\pi}{2}(h - 4k\delta'')\right] + \cos\left[\frac{\pi}{2}(4h\delta'' + k)\right]\right\}. \quad [1]$$

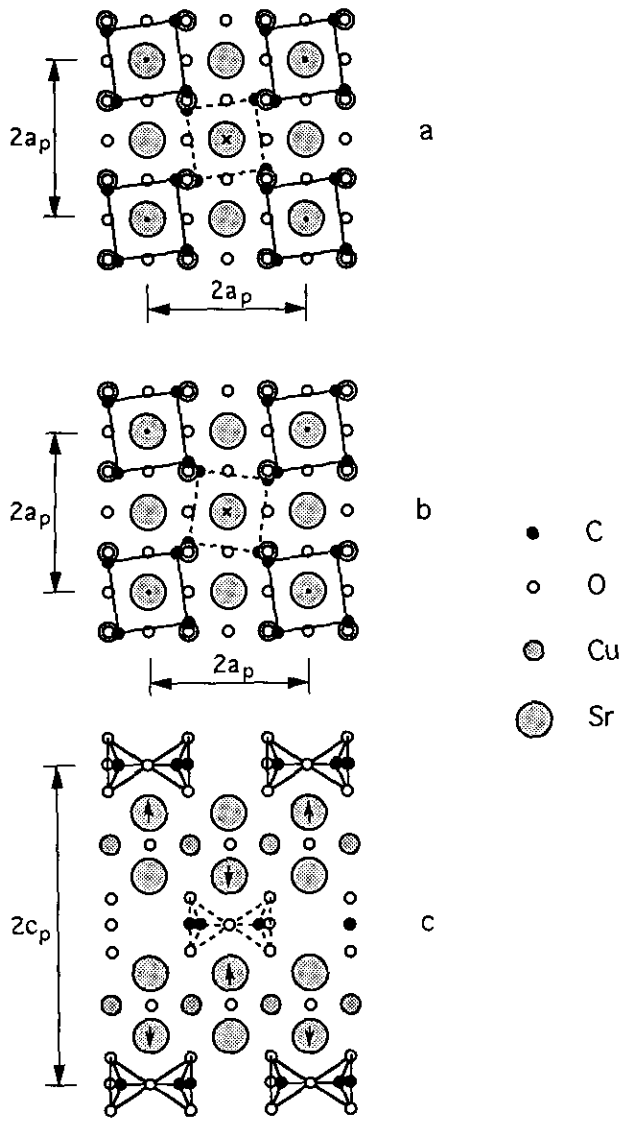

FIG. 5. Schematic structures of the $Sr_2CuO_2(CO_3)$ superlattice unit cell: (a) projection along [001] direction of the body centered lattice variant. The CO_3 arrangement consisting of the same type of CO-loops in the top, mid, and bottom layers, is emphasized by the full line squares in the top layer, and by the broken line square in the mid layer; (b) projection along [001] direction of the primitive lattice variant. The CO_3 arrangement consisting of two types of CO-loops: + loops in the top and the bottom layers, and − loops in the mid layer, is emphasized as in (a); (c) the projection along [100] direction for both lattice variants. The CO_3 arrangement is emphasized. The displacements of Sr atoms are indicated by small arrows in (c) and by dots or crosses in (a) and (b) in the large circles which represent the Sr atoms; shaded and small open circles represent Cu and O atoms, small black circles represent C atoms, respectively.

For a − loop, represented in Fig. 4a, the atom positions can be obtained by changing δ' into $-\delta'$, and δ'' into $-\delta''$, in Fig. 4c, respectively. The structure factors F for the − loop, refered to the same reference system are then obtained by the substitution $\delta'(\delta'') \rightarrow -\delta'(-\delta'')$ in [1].

For the special case (i): ($\delta' = \frac{1}{4}$; $\delta'' = \frac{1}{12}$) the structure factor F becomes:

$$F = 2f_C\left\{\cos\left[\frac{\pi}{2}(h-k)\right] + \cos\left[\frac{\pi}{2}(h+k)\right]\right\} + 2f_O\left\{\cos\left[\frac{\pi}{6}(3h-k)\right] + \cos\left[\frac{\pi}{6}(h+3k)\right]\right\} \quad [2i]$$

while for the special case (ii): ($\delta' = \frac{1}{6}$; $\delta'' = 0$) the structure factor F becomes:

$$F = 2f_C\left\{\cos\left[\frac{\pi}{6}(3h-2k)\right] + \cos\left[\frac{\pi}{6}(2h+3k)\right]\right\} + 2f_O\left\{\cos\left(\frac{\pi h}{2}\right) + \cos\left(\frac{\pi k}{2}\right)\right\}. \quad [2ii]$$

The structure factor for the spatial arrangement of the CO layers in the unit cell is then:

$$F = F^{(+)} + F^{(+)}\exp[\pi i(h+k+l)] \quad [3]$$

when assuming that the CO loops in successive layers have the same sign (Figs. 5a and 5c), and hence that the lattice is body centered (I). If the CO loops are assumed to have opposite signs in successive layers (Figs. 5b,c), the structure factor becomes:

$$F = F^{(+)} + F^{(-)}\exp[\pi i(h+k+l)]. \quad [4]$$

The lattice is now primitive (P).

When considering the expressions [1] and [2i,ii] it becomes evident that $F^{(+)}$ and $F^{(-)}$ become identical for particular types of reflections in the general case, as well as in the special cases: (i) and (ii). This is summarized in the following table:

Reflections		Relations
$h\ 0\ 0$		$F^{(+)} = F^{(-)}$
$h\ 0\ l$		$F^{(+)} = F^{(-)}$
$0\ k\ l$		$F^{(+)} = F^{(-)}$
$h\ h\ l$		$F^{(+)} = F^{(-)}$
$h\ k\ 0$		$F^{(+)} \# F^{(-)}$
$h\ 2h\ l$	$h = 1$	$F^{(+)} \# F^{(-)}$
$h\ 2h\ l$	$h = 2$	$F^{(+)} = F^{(-)}$
$h\ 3h\ l$	$h = 1$	$F^{(+)} = -F^{(-)}$
$h\ 3h\ l$	$h = 2$	$F^{(+)} = F^{(-)}$

It thus turns out that in projection along a number of simple zones such as [100], [010], and [110], the + loops and − loops have the same structure factor independent of the particular choice of δ' ($\frac{1}{6} < \delta' < \frac{1}{4}$) and δ'' ($0 < \delta'' < \frac{1}{12}$). This is also intuitively evident since the projections of

their structures along these special zones are identical. In the diffraction pattern as well as in the image along such zones no difference will be noted between the two possibilities [3] and [4]. The patterns along such zones are consistent with a body centered lattice (Figs. 1a,b). The patterns along more complex zones such as $[2\bar{1}0]$ and $[3\bar{1}0]$ (Fig. 3) show that if both types of CO loops are present in the structure, the additional spots may appear at the locations forbidden by the body centered lattice; the lattice may also be primitive, however.

Although this conclusion is based on the CO sublattice only, it applies to the complete structure because the CO sublattice is the symmetry determining one; it reduces the overall symmetry to a subgroup of that of the perovskite block.

We now show in some more detail that the appearance of the streaked spots corresponds with the presence of the primitive unit cell $2a_p \times 2a_p \times 2c_p$.

As mentioned above the $(h0l)^*$, [or $(0kl)^*$] and $(hhl)^*$ sections in Fig. 1 are consistent with the body centering, but the $(hk0)^*$ and $(hkl)^*$ sections for $h \neq k$ in Figs. 1c and 3, respectively, are not. The reason is that along the former three zones the structure factors of the + loop and − loop are the same, but not along the latter two zones.

We show further that the observed spot patterns in Figs. 3a,b, along the zones [310] and [210] are consistent with a primitive lattice. The structure factor of the primitive structure can be written as [4].

For reflections of the type $h\ 2h\ l$ this leads to $F = F^{(+)} + F^{(-)}$, for $h = 1$, $l =$ odd, and $h = 2$, $l =$ even, and to $F = F^{(+)} - F^{(-)}$ for $h = 1$, $l =$ even, and $h = 2$, $l =$ odd. We conclude that all reflections should be present in the $[h\ 2h\ l]^*$ rows of reflections in accordance with the observations. We note that $F = F^{(+)} - F^{(-)}$ for the diffuse reflections. The latter would thus be absent (Fig. 3c) if only one type of CO loop is present, i.e., if the lattice becomes body centered.

For reflections of the type $h\ 3h\ l$ we find that $F = F^{(+)} + F^{(-)}$ for $l =$ even and $F = F^{(+)} - F^{(-)}$ for $l =$ odd. This leads in the row $[13l]^*$ to extinction for $l =$ even from Eqs. [1] and [4] and to $F = 2F^{(+)}$ for $l =$ odd, when taking into account the set of relations in the table. In the row $[26l]^*$ we have $F = 2F^{(+)}$ for $l =$ even and $F = 0$ for $l =$ odd. The presence of sharp spots with $l =$ even in the $[13l]^*$ superlattice row is not predicted as a contribution of the primitive CO superlattice but it is consistent with spots due to the puckering of the SrO layers which results in a body centered lattice of the underlying SrO–CuO_2–SrO block layer structure, as discussed in section 4. The body centered CO superlattice cell would also contribute to these sharp spots in the $[13l]^*$ superlattice row since $1 + 3 + l =$ even if $l =$ even.

From this discussion we can conclude that all spots due to a body centered structure are always present as sharp spots, but that additional, streaked spots, which are only consistent with a primitive lattice, also appear. This means that in certain crystal parts which exhibit only a body centered lattice, the CO sublattice is either highly disordered or very well ordered, containing only one type of CO loop, with the same space group $I4$ as the underlying block-layer structure, in accordance with the proposal in Ref. (4). However, in other crystal fragments well ordered CO loops of two types alternate in successive layers and a primitive CO lattice appears superimposed on the body centered structure of the SrO–CuO_2–SrO block layer. The unit cell of this primitive CO-lattice is of the same size: $2a_p \times 2a_p \times 2c_p$ as that of the body centered block layer lattice. In this latter case the reflections which violate the body centered diffraction conditions, i.e., those with $h + k + l =$ odd are streaked to various degrees or consist of a cluster of weak closely spaced discrete spots (Fig. 3d), reflecting the degree of local order in the CO layer structure.

6. ORIGIN OF THE DIFFUSE SCATTERING

As pointed out above the diffraction patterns exhibit diffuse streaks along $\mathbf{c}^*$ in the $[2\bar{1}0]$ and $[3\bar{1}0]$ zones for which $h + k + l =$ odd. No diffuse scattering is observed in the $(0kl)^*$ or $(h0l)^*$ sections since for all spots in these sections $h + k + l =$ even. Also in the $(hk0)^*$ section no streaks are visible because they are perpendicular to this section. They may nevertheless possibly contribute to the intensity of the very weak spots for which $h + k + l =$ odd. The streaking of the $[00l]^*$ rows in the $[2\bar{1}0]$ and $[3\bar{1}0]$ zone patterns is due to double diffraction as pointed above.

The observed streaking is characteristic of one-dimensional planar disorder. We already pointed out that any disorder must be located in the CO layers since there is considerable freedom in the positioning of the CO loops.

The following model accounts for the diffuse scattering:

Let the "normal," or reference structure be based on a primitive lattice. This is justified because of the presence of spots with $h + k + l =$ odd observed in the $[2\bar{1}0]$ and $[3\bar{1}0]$ zones. This implies that in successive CO layers the CO loops are of opposite sense as in Fig. 5b. The structure in which all CO layers contain loops of the same sense, and which is thus body centered, must have a comparable stability and may thus occur as an intergrowth with the primitive structure. In the sequence of layers of + loop, centered on the origin, alternating with layer of − loop centered on $\frac{1}{2}\frac{1}{2}\frac{1}{2}$ one can imagine a stacking fault, i.e., a + loop layer centered on 000 followed by a + loop layer centered on $\frac{1}{2}\frac{1}{2}\frac{1}{2}$. The fault vector $\mathbf{R}$ of such a fault is $\mathbf{R} = \frac{1}{2}[111]$, which is a lattice vector for the body centered perovskite sublattice of the block

layer structure, but not for the primitive lattice of the CO layer structure. The reflections $\mathbf{g}$ for which $\mathbf{g} \cdot \mathbf{R} = \frac{1}{2}(h + k + l) =$ fractional, would then become streaked. This is precisely the case for all streaked reflections; it is therefore clear that the CO layer structure must be a mixture of the primitive and the body centered structure.

Conversely, the observed streaked reflections strongly suggest a fault vector $\mathbf{R} = \frac{1}{2}[111]$. Such a vector is a lattice vector in the body centered superlattice and thus does not lead to streaking of the spots with $h + k + l = 2n$. This remark supports our assumption that in samples exhibiting streaked reflections the reference structure of the CO layers is the primitive one, rather than the body centered one.

Since there are two energetically almost equivalent stacking modes it is possible to imagine complicated long period stacking sequences. This may explain the occurrence of sequences of equidistant sharp spots present in the streaks in the diffraction patterns of Fig. 3.

7. STACKING MODES

The diffraction phenomenon are clearly in agreement with the occurrence of two basic stacking modes leading to either a primitive or a body centered lattice, with the same unit cell. We can distinguish two different stacking positions A and B for the CO layers. In A the centers of the CO loops project in the origin of the unit cell, whereas in B the centers of the CO loops project in the $\frac{1}{2}\ \frac{1}{2}\ 0$ positions. The two patterns can further consist of either + loop or − loop. The body centered stacking can then be represented by the symbol

$$\cdots A^+B^+A^+B^+ \cdots \text{ (or } \cdots A^-B^-A^-B^- \cdots).$$

The primitive structure is similarly represented by the symbols:

$$\cdots A^+B^-A^+B^- \cdots \text{ (or alternatively } \cdots A^-B^+A^-B^+ \cdots).$$

Since both fundamental stacking modes are energetically very nearly equivalent, stacking faults and alternative stacking sequences are to be expected.

The stacking faults with a displacement vector $\mathbf{R} = \frac{1}{2}[111]$ can only occur in the primitive structure. Using the described symbolism, such a fault can be represented as:

$$\cdots A^-B^+A^-B^+\underline{A}^-\underline{B}^-A^+B^-A^+B^- \cdots. \qquad [5]$$

The shift over $\mathbf{R}$ interchanges A and B, without affecting the sense of the layer and extracts one layer. Applying this algorithm to sequence [5], restores the perfect structure.

It is clear that the body centered structure does not allow this type of fault since the translation $\mathbf{R}$ is then a lattice vector. This is consistent with the observation that only spots characteristic of the primitive structure are streaked. Regular sequences of "faults" may result in long period structures such as the four layer structure:

$$\cdots A^-B^+A^+B^-/A^-B^+A^+B^-/ \cdots.$$

The closely spaced equidistant spot sequences (Fig. 3) in the $[3\bar{1}0]$ and $[2\bar{1}0]$ zones centered on all positions characteristic for the primitive lattice, are satellites of these spots; their geometry (Fig. 3d) suggests a superstructure with a spacing $c \approx 10$–$11\ c_p$. The precision of the measurement does not allow to conclude unambiguously whether or not the long spacing is commensurate or noncommensurate with the basic spacing c_p. The satellite sequences centered on spots with $l =$ odd (e.g., on 135, indicated by arrowhead in Fig. 3d) are fractionally shifted over $\frac{1}{2}$ of the distance between the satellites, whereas those centered on spots with $l =$ even do not exhibit a shift. Such a diffraction pattern can be attributed to a long period interface modulated superstructure of the primitive structure, the interfaces being of the type discussed above, i.e., having a translation vector $\mathbf{R} = \frac{1}{2}[111]$. The fractional shifts which are given by $\mathbf{g} \cdot \mathbf{R}$ are then $\frac{1}{2}$ if $l =$ odd and 0 when $l =$ even, as observed. The spacing of the satellites leads to an average separation of the interfaces between $5c_p$ and $6c_p$. Possible concrete models of the long period structure can be represented by stacking symbols such as:

$$\cdots A^-B^+/A^+B^-A^+B^-A^+/B^+A^-B^+A^-B^+/A^+B^- \cdots \text{ or}$$
$$\cdots A^+B^-A^+B^-A^+/B^+A^-B^+A^-B^+A^-/B^-A^+B^- \cdots.$$

Other potential faults vectors, which could also occur in the body centered structure are $\frac{1}{2}[101]$ or $\frac{1}{2}[011]$. These vectors are lattice vectors of the perovskite block, but not for the CO layers. Such faults would lead to diffuse streaks at positions for which $h + l =$ odd or $k + l =$ odd, respectively. Such diffuse spots have not been observed, however, suggesting that only the two relative stacking positions described above, and which maintain the quasi-tetragonal symmetry, actually occur.

8. HIGH RESOLUTION IMAGING

The above discussion in section 7 has lead to the conclusion that the ordering of the superstructure has to be sought in the atomic arrangement of the CO loops within the CO layers and in the stacking of the CO layers. In the perovskite blocks with a lattice parameter of ≈0.39 nm the heavy atom columns can rather easily be revealed along simple zones such as [100], [110], and [001], but such images are not likely to provide any relevant infor-

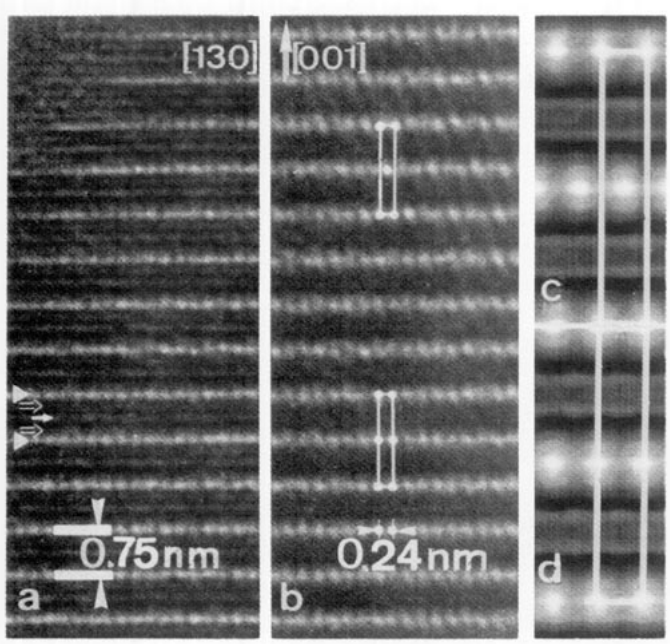

FIG. 6. High resolution images of $Sr_2CuO_2(CO_3)$ along the oblique zone [130]: (a) thin area of wedge shaped crystal; only the CO_3 layers produce bright dot rows, marked by triangles on the left margin, while the CuO_2 and Sr layers are represented by continuous fringes (indicated by full arrow and open arrows, respectively); (b) thicker area of the same crystal; note the vertical and staggered stacking of bright dots along [001] direction indicated by rectangles in the lower and upper part, respectively; (c) simulated image of the primitive lattice cell along [130] direction displaying staggered arrangement of bright dots representing columns of CO-loops; (d) simulated image of the body-centered lattice cell along [130] direction displaying vertical arrangement of bright dots. Magnification of the simulated images in (c) and (d) is three times larger than of the images in (a) and (b).

mation on the superstructure since along these zones the contrast of the weakly scattering carbon atoms will be negligible as compared to the contrast due to the heavy atoms. On the other hand, those sections of reciprocal space which contain a large fraction of intense, purely superstructure reflections, corresponding to a resolvable spacing and which moreover, contain only basic perovskite spots leading to unresolved fringe spacings, are likely to be the most relevant ones (10). The atomic column separations for the perovskite block are then too small to be resolved in the microscope. Such a technique was already used in the study of the Ga-12n2 and Co-1212 compounds (11, 12). Under these conditions the superperiod can be revealed as an array of dots against a more or less continuous background. The [$3\bar{1}0$] zone in Fig. 3a is such a reciprocal lattice section and Figs. 6a,b are the corresponding images. Only one family of lines of bright dots is visible out of the bands of three almost continuous fringes perpendicular to c, in the thin specimen area in Fig. 6a. The spacing between the bright lines is consistent with the c_p spacing of the basic perovskite structure; i.e., it is 0.75 nm $\approx c_p$. Image simulations (Figs. 6c,d), based on the idealized model described above, have shown that these bright dot lines, which are clearly revealed in the area of larger specimen thickness (Fig. 6b), represent the CO layers; this is also the case for the simulation based on the structural model in which a displacement modulation of the strontium positions was implemented (10) to take into account for the variety of the Sr–CO loop configurations pointed out in Section 4. These simulation results confirm the remark that the CO layer is the only one that produces a resolvable spacing along this direction. The dot spacing of ≈0.24 nm is consistent with the d^{s}_{310} spacing of the superstructure. The corresponding spacing in the basic perovskite layers is $d^{p}_{310} \approx 0.12$ nm and it remains unresolved under the imaging conditions of Fig. 6. The bright dots form a rectangular mesh and are vertically arranged along the [001] direction (lower part of Fig. 6b), except for some faults where a staggered arrangement is noted (this is indicated in the upper part of Fig. 6b). Whatever be the atom columns corresponding to the bright dots, the observation proves that the CO layer is ordered and it determines the $2a_p \times 2a_p$ unit mesh; it confirms our models for the superstructure which have to be associated with ordering in the CO layers (Figs. 4 and 5). A model whereby the CO_3 groups would be oriented at random as proposed in (3, 6) can only be considered as the first, rough, approximation.

A detailed interpretation of the image can be deduced from image simulation. As superstructure models for the simulation we used the complete structure consisting of the sublattice of perovskite SrO-CuO_2-SrO block-layers and of the superlattice of CO-loops (Fig. 5); for the primitive superstructure: an alternating stacking of "+ loops" and "− loops" in successive CO-layers (Fig. 5b,c); for the body-centered superstructure: a stacking of one type ("+") of CO-loops in successive CO-layers (Fig. 5a,c). The simulated image along the [130] zone of the primitive lattice is characterized by a staggering array of dots (Fig. 6c) while in the simulated image of the body-centered lattice, the array of dots is stacked vertically (Fig. 6d).

9. DISCUSSION

The observation of the primitive structure next to the body-centered one has some implications concerning the structure of $Sr_2CuO_2(CO_3)$ as proposed previously in (4). In that structure, the CuO_6 octahedra, which are connected by their corners in the CuO_2 layer, have been assumed to be deformed as well as the CO_3 triangles, which therefore deviate from an equilateral shape. However, the Debye–Waller factors of the oxygen atoms corresponding to the CO_3 triangles and to the apices of CuO_6 octahedra remained large (4). The two deformations seem to some extent to be imposed by the assumption

that the carbon, as well as the copper atoms tend to be aligned along the c axis. The deformation pattern of the CuO_6 octahedra and the corresponding puckering of the Sr layers result in the body centered structure. Within the model proposed here this means that the CO loops have to be all oriented in the same sense in all the CO layers in accordance with the body centered lattice (4). Since we have presented evidence that also a primitive lattice occurs, containing CO loops of opposite sense in successive CO layers, the deformation pattern in this structure, in particular the tilts, ought to be in the opposite sense for a given layer of CuO_6 octahedra. This would presumably cause the octahedra to be less deformed and also allow the CO_3 triangles to maintain a more regular, equilateral shape, as assumed in our idealized structure model. It has to be pointed out that in this idealized structure, the C–O bond lengths in the CO_3 groups are equal to the usual bond lengths realized in calcite and other carbonates (13, 14), and that the height of the equilateral CO_3 triangle is exactly half of the perovskite lattice parameter as it is schematically shown in Fig. 4; therefore: $d_{C-O} = 0.129$ nm $= \frac{1}{3} a_p$. In this idealized structure, free of the deformation of the perovskite polyhedra, the two above mentioned arrangements of CO_3 groups forming + loops and − loops respectively, are energetically equivalent. It is therefore felt that this idealized structure model may explain the details of our observations.

However, the idealized model presented here is hardly to be expected in the real structure. Point defects either in the CO layer (O or C vacancy, or Cu substitution for C), or in the Sr layer (substitution of Ba for Sr) would induce disorder, the relaxation displacements of light carbon and oxygen atoms surrounding a defect. The partial substitution of Sr by Ba in $(Sr/Ba)_2CuO_2(CO_3)$ probably prevents ordering in CO layers due to difference in Sr–Ba atomic sizes, inducing disorder in the orientation of the planes of the CO_3 group. This could explain the results of the structure determination for the $(Sr/Ba)_2CuO_2(CO_3)$ compounds where no such a superstructure were found (8, 9, 15). One can speculate whether or not pure $Sr_2CuO_2(CO_3)$ would be superconductive in highly disordered regions as it was suggested for regions with defects in $(Sr_{1-x}Ca_x)_{1-y}CuO_2$ (16).

The electron irradiation (400 kV) in the microscope disorders preferentially the C sublattice by displacement damage since carbon is the lightest atom in the structure. This is consistent with the disappearance of the superlattice spots after prolonged irradiation and is consistent with the assumption that the superperiod is primarily due to the arrangement of CO loops and not to an accompanied deformation pattern of CuO_6 octahedra.

Fading out of the primitive lattice spots after prolonged electron irradiation indicates the destruction of the long range order, not only between the CO layers, but also within the CO layers. It is obvious that both types of CO loops superstructures, primitive and body centered are to the same extent susceptible to the electron damage. However with increasing disorder first the sense of the CO loops will be lost and the structure will thus tend to become body centered: $I4$. Since the displacement modulation of the Sr sublattice, leading to puckering of these layers and to body centering (and to the doubling of the perovskite unit mesh), is coupled to the degree of order in the CO layers, it will also tend to disappear with increasing disorder in the CO layers. This allows to understand why in some cases, an apparently higher symmetry $Pmmm$ and a perovskite unit mesh was found (3, 6).

ACKNOWLEDGMENTS

O. Milat gratefully acknowledges the commission of EC, DG XII, for the Grant S/CII*-913167. The work has been performed in the framework of a UIAP-11 contract with Ministery of Science Policy and with financial support of Belgian National Science Foundation (NFWO) and National Impulse Programme on High T_c Superconductivity (SU/03/17).

REFERENCES

1. Y. Tokura, *Physica C* **185–189,** 174 (1991).
2. Hk. Muller-Buschbaum, *Angew. Chem. Int. Ed. Engl.* **28,** 1472 (1989).
3. T. G. N. Babu, D. J. Fish, and C. Greaves, *J. Mater. Chem.* **1,** 677 (1991).
4. Y. Miyazaki, H. Yamane, T. Kajitani, T. Oku, K. Hiraga, Y. Morii, K. Fuchizaki, S. Funahashi, and T. Hirai, *Physica C* **191,** 434, (1992).
5. K. Kinoshita and H. Yamada, *Nature* **357,** 313, (1992).
6. Y. Tokura, H. Takagi, and S. Uchida, *Nature* **337,** 345 (1989).
7. O. Milat, G. Van Tendeloo, J. Van Landuyt, and S. Amelinckx, in preparation.
8. A. R. Armstrong and P. P. Edwards, *J. Solid State Chem.* **98,** 432, (1992).
9. C. Chaillout, Q. Huang, R. J. Cava, J. Chenavas, A. Santoro, P. Bordet, L. J. Hodeau, J. J. Krajewski, J. P. Levy, M. Marezio, and W. F. Peck, Jr, *Physica C* **195,** 335 (1992).
10. O. Milat, G. Van Tendeloo, J. Van Landuyt, and S. Amelinckx, submitted for publication.
11. O. Milat, T. Krekels, G. Van Tendeloo, and S. Amelinckx, *J. Phys. I Fr.*, to appear.
12. T. Krekels, O. Milat, G. Van Tendeloo, S. Amelinckx, T. G. N. Babu, A. J. Wright, and C. Greaves, *J. Solid State Chem.*, to appear.
13. R. L. Sass, R. Vidale, and J. Donohue, *Acta Crystallogr.* **10,** 567 (1957).
14. P. C. Healy and A. H. White, *J. Chem. Soc. Dalton Trans* 1913 (1972).
15. F. Izumi, K. Kinoshita, Y. Matsui, K. Yanagisava, T. Ishigaki, T. Kamiyama, T. Yamada, and H. Asano, *Physica C* **196,** 227 (1992).
16. M. Azuma, Z. Hiroi, M. Takano, Y. Bando, Y. Takeda, *Nature* **356,** 775 (1992).